Available online at www.sciencedirect.com
ScienceDirect
Polymer 48 (2007) 5208–5218
polymer
www.elsevier.com/locate/polymer

# Design of polymer nanofiber systems for the immobilization of homogeneous catalysts – Preparation and leaching studies

Michael Stasiak [a], Caren Röben [b], Nadine Rosenberger [b], Florian Schleth [b], Armido Studer [b], Andreas Greiner [a], Joachim H. Wendorff [a,*]

[a] *Department of Chemistry, Philipps-Universität Marburg, Hans-Meerwein-Strasse, 35032 Marburg, Germany*
[b] *Institute of Organic Chemistry, Westfälische Wilhelms-Universität Münster, Corrensstrasse 40, 48149 Münster, Germany*

Received 3 November 2006; received in revised form 11 May 2007; accepted 3 July 2007
Available online 12 July 2007

**Abstract**

In this paper a novel general concept for the immobilization of catalysts is presented. It will be shown that catalysts covalently bound to low-molecular weight polystyrene ($M_n > 4000$ g/mol) can be immobilized into high molecular weight polystyrene nanofibers using the electrospinning process. The immobilized catalyst–oligostyrene conjugates are well dispersed within the fibers as shown by DSC and X-ray studies. In DMSO, the oligostyrene tails of the catalysts suppress the leaching of the catalysts out of the fibers into the solution for thermodynamic reasons. Leaching studies are conducted using naphthalene-conjugated oligostyrenes using fluorescence spectroscopy. The naphthalene–polystyrene conjugates with defined molecular weight are readily prepared using nitroxide-mediated radical polymerization (NMP). As a model catalyst system, proline–polystyrene conjugates are synthesized by NMP to study catalyst leaching out of the polystyrene nanofibers used as a catalyst matrix.


*Keywords:* Nanofibers; Controlled radical polymerization; Catalytic activity

## 1. Introduction

The immobilization of catalysts is a concept which has been exploited in heterogeneous catalysis. In heterogeneous catalysis catalysts are immobilized on porous carriers including zeolithes, porous aluminum oxide particles, titanium dioxide, graphite with great success [1,2]. Immobilization on porous substrates allows in this case controlling the specific surface area, the accessibility of the catalyst and in certain cases even the catalytic activity for the particular case that the electronic state of the catalyst is modified due to the contact with the materials used for immobilization. A further advantage is that immobilization allows the retrieval of the catalyst for the reaction mixture to a very high percentage.

Concepts aiming at the immobilization of homogeneous catalysts seem to be in contradiction to the very nature of homogeneous catalysis which is characterized by a molecular dispersion within the reaction mixture, in general in solution or melt. Yet such an immobilization would have definite advantages. The separation of the catalysts from the product is a major problem and this is of particular significance in the synthesis of pharmaceutical, microelectronic or optoelectronic compounds which should ideally be completely free of catalysts. Furthermore as one goes from batch reactions to continuous reactions – microreaction techniques being examples in case [3] – one faces the problem of keeping the catalyst in the reaction vessel while the reaction components flow through the reactor. Finally the possibility to re-use the homogeneous catalysts as completely as possible is also an important and an economic topic.

In fact, microencapsulation approaches for homogeneous catalysts based on polymers have been reported in the literature [4,5]. A typical approach consisted in dispersing the

* Corresponding author.
*E-mail addresses:* studer@uni-muenster.de (A. Studer), wendorff@staff.uni-marburg.de (J.H. Wendorff).

0032-3861/$ - see front matter © 2007 Elsevier Ltd. All rights reserved.
doi:10.1016/j.polymer.2007.07.006

powdered catalyst in a polymer solution and inducing subsequently a phase separation by suitable means such as a temperature drop. The powdered catalyst is covered in this case by a thin polymer layer which can be hardened by solvent treatment. Sc, Os, Pd and Ru catalysts were considered for instance. Polystyrene (PS) has been found to be the polymer material of choice. PS obviously provides specific interactions with such catalysts reducing leaching.

It is important to point out that a molecular dispersion has not been achieved in this type of immobilization but rather a microparticle dispersion of the homogeneous catalyst within the particular carrier system. One consequence is that the concentration of the catalysts has to be high and that the yield often does not amount to 100%. Homogeneous catalysts have furthermore been immobilized for instance by attaching them via coordinate or covalent bonds to a support [6]. It is, however, a frequent observation that the effectiveness of the catalyst is strongly reduced by this approach towards immobilization.

A molecular dispersion of a homogeneous catalyst within a carrier, in which (i) the components of the reaction mixture are able to diffuse in and out, (ii) the catalyst remains confined yet, (iii) the catalyst is able to perform translational and rotational motions, at least on a local scale, should not really restrict the catalytic activity of a given homogeneous catalyst. It is obvious that zeolithes, aluminum oxide and similar immobilizing systems used in heterogeneous catalysis can, in general, not be used for this purpose. Synthetic polymers, on the other hand, have distinct advantages for such applications. This paper is concerned with the design of polymer based immobilization systems for homogeneous catalysts. The preparation of polystyrene fibers containing polystyrene–naphthalene conjugates and proline–polystyrene conjugates by the electrospinning process will be presented. In addition, leaching studies of the polystyrene conjugates out of the polystyrene fibers will be discussed. These leaching studies are highly important for future application of this novel immobilization concept in homogeneous catalysis.

## 2. Concept considerations

### 2.1. Design of the polymer carrier system

It is well documented that polymers are excellent choices as host matrices for guest–host systems designed, for instance, for nonlinear optical applications, light emitting diodes, information storage, etc. [7–9]. Polymers commonly dissolve organic, metal organic, liquid crystalline, etc. low molar mass and oligomeric compounds up to high concentrations and this holds not only for the molten but also for the solid glassy or partially crystalline state. Atactic polymers such as polystyrene or polymethylmethacrylate are solid glasses at room temperature. Yet due to local molecular motions present even in the solid glassy state – or the partially crystalline state for that matter – the guest molecules are able to perform rotational and translational motions with the glassy matrix and solvents or functional molecules are able to perform diffusional motions in such solid matrices [9,10]. All these arguments imply that polymers might be used in homogeneous catalysis as carriers which do not destroy the nature of the homogeneously catalyzed reaction. The possible preparation of products with strongly reduced catalyst contamination or even free of catalysts is a major benefit. Yet there may be even further benefits. The polymer carrier may provide specific dynamic environments affecting the reactions such as chiral environments [11].

An important feature which will strongly affect the efficiency of the catalytic system is its architecture. It should be structured in any case on a nanoscale since such a scale reduces the time required for the compounds of the reaction mixture to diffuse towards the catalysts within the carrier. Polymer nanoparticles, thin films, porous membranes composed of polymers are possible architectures. Yet it seems that fibers assembled as nonwovens offer distinct advantages. Nonwovens composed of polymer fibers are used extensively for filtering gaseous and fluid media which are pumped through [12–14]. A large number of experimental and theoretical papers have dealt with the internal specific surface, the intrinsic pore sizes, the probability of the particles of the fluids or gases within the nonwoven to impact on the nanofibers in the pores, with the permeability of such nonwovens as a function of the orientation of the fiber in space – 1-, 2-, 3-dimensional – as well as with their total porosity, a key parameter being the fiber diameter [15–17]. These simulations as well as corresponding experimental results clearly show that such nonwoven display features coming close to those of highly porous membrane structures of the type discussed above for heterogeneous catalysis in terms of pore size, internal surface, permeability provided that they are made from nanofibers. The advantage of the approach based on nonwovens is that they can be manufactured on a large scale from a large variety of polymers. Furthermore, aggregation effects, a problem for the microencapsulated catalysts of the fibers reducing the transport processes can be avoided by suitable fiber textures such as, for instance, a random nonwoven texture. The technique of choice for nonwovens based on nanofibers is electrospinning [12–14].

### 2.2. Design of the model catalyst system

In a previous paper we were able to demonstrate that a homogeneous catalyst can be immobilized within polymer nanofibers without loss of its activity. Core/shell polymer nanofibers were used for the immobilization of scandiumtriflate and imino aldol and aza-Diels–Alder model reactions were investigated [18]. It was observed that the catalyst is much more active in this case compared to the case of an immobilization in microspheres or even to the case of a reaction in solvents. Yet the leaching of the catalyst into the carrier environment turned out to be a major problem. The reason for the leaching evidently is that the catalyst considered was soluble within the solvent used for the reaction.

The concept thus has to be to prepare a catalytic system which can be homogeneously dispersed within the polymer matrix yet which is strongly insoluble in the solvents used

for the reaction. The efficiency of the catalyst can be enhanced by designing the catalyst in such a way that it is able to perform rotational and translational motions within the matrix, in close agreement with the corresponding dynamics in the solvent and in such a way that it has a tendency to enrich in the surface regions of the fibers. Shorter diffusion distances and higher local concentrations of the catalyst are the consequences.

A convincing choice for such a catalytic system is the one in which the target catalyst is attached to an oligomer chain having the same chemical composition as the matrix polymer. The oligomer chain can react as plasticizer, it is able to perform diffusional motions within the polymer matrix and it tends to enrich at the surface of the polymer matrix. All these features, i.e. solubility in the reaction solvent, the diffusion within the entanglement network of the matrix and the enrichment, are strongly dependent on the oligomer chain length. The solubility of the catalyst attached to the oligomer chain decreases with increasing molecular weight, the enrichment is larger for smaller chain length and the diffusion is reduced with increasing chain length particularly if the oligomer chain length surpasses the entanglement chain length. The oligomer chain length is thus the parameter which allows optimizing the catalytic system. We have selected polystyrene as carrier polymer and oligostyrene-modified proline of different chain lengths as the model catalysts. To investigate the solubility of the oligostyrene system in the reaction solvents via spectroscopic studies we used oligostyrene-modified chromophores characterized also by different chain lengths.

## 3. Experimental

### 3.1. General

$Cu(OTf)_2$ (ABCR, 98%), 2,2,6,6-tetramethylpiperidin-4-methoxy-*N*-oxyl radical (Degussa AG, 98%), Cu powder (ACROS, 99%), (4,4′-di-*tert*-butyl)-2,2′-bipyridine (Aldrich, 98%), *n*-butyllithium (ACROS, 1.6 M in hexane), trifluoroacetic acid (Merck, ≥99%), $LiAlH_4$ (Merck, 97%), $CBr_4$ (Aldrich, 99%) and triphenyl phosphine (Fluka, ≥95%) were used as received. Styrene (BASF, 99%) was distilled from $CaH_2$ under reduced pressure to remove the stabilizer and was stored at 4 °C under an argon atmosphere. Dichloromethane (DCM) was distilled from phosphorous pentoxide, *N*,*N*-dimethylformamide (DMF) was distilled from $CaH_2$, and tetrahydrofuran (THF) was distilled from potassium before use. Benzene was distilled from sodium.

$^1H$ NMR (500 MHz, 400 MHz, 300 MHz) and $^{13}C$ NMR (125 MHz, 100 MHz, 75 MHz) spectra were recorded on a AMX 500 (Bruker), ARX 300 (Bruker) or ARX 200 (Bruker). Chemical shifts $\delta$ were measured in ppm relative to $SiMe_4$ as internal standard. TLC: silica gel *60* $F_{254}$ plates (Merck), detection with UV or dipping into a solution of $KMnO_4$ (1.5 g in 333 mL of 1 M NaOH) or a solution of $Ce(SO_4)_2 \cdot H_2O$ (10 g), phosphomolybdic acid hydrate (25 g), concentrated $H_2SO_4$ (60 mL) and $H_2O$ (940 mL), followed by heating. Flash chromatography (FC): silica gel 60 (40–60 μm, Merck or Fluka) at 0.1–0.4 bar. Melting points: SMP 10 (Bibby-Stuart Scientific), uncorrected. IR spectra were recorded on a Digilab FTS 4000 equipped with an MKII Golden Gate Single Reflection ATR System, an IR 750 (Nicolet Magna), or an *IFS-200* (Bruker). ESI-MS and HRMS were performed using a Bruker MicroTof. Elemental analysis was performed using a Vario EL III (Elementar). Size exclusion chromatography (SEC) was carried out with THF as eluent at a flow rate of 1.0 mL/min at room temperature on a system consisting of an L-6200A Intelligent Pump (Merck Hitachi), a set of two PLgel 5 μm MIXED-C columns (300 × 7.5 mm, Polymer Laboratories, linear range of molecular weight: 200–2 000 000 g/mol), and a Knauer Differential refractometer ($\lambda = 950 \pm 30$ nm) detector. Data were analyzed with PSS WinGPC compact V 7.20 software based upon calibration curves built upon polystyrene standards (Polymer Laboratories polystyrene medium MW calibration kit S-M-10) with peak molecular weights ranging from 500 g/mol to 3 000 000 g/mol.

The X-ray analysis was performed with a Siemens D 5000 wide-angle goniometer. Scanning electron microscopy was performed with a Hitachi S-4100 microscope using an acceleration voltage of 10 kV. Differential scanning calorimetry was performed using a Mettler Toledo DSC 821 with a heating rate of 10 K/min. Samples were heated and cooled down twice in the range of 20–200 °C. The second heating curves have been used for analysis. For UV/Vis-spectroscopic investigations a 500 W Xenon arc lamp, monochromators from Acton Research Corporation of type SP 300 i, synthetic fused silica lenses from Melles Griot, a Photomultiplier (type R 928) and Photoncounters (type R 4632) from Hamamatsu were used.

### 3.2. Synthesis of the oligostyrene–naphthalene and oligostyrene–proline conjugates

#### 3.2.1. 2,2,6,6-Tetramethyl-1-(1-naphthalen-2-yl-ethoxy)-piperidine (*2*)

2-(1-Bromo-ethyl)-naphthalene **1** (1.60 g, 6.80 mmol, 1.00 equiv.), 2,2,6,6-tetramethylpiperidin-4-methoxy-*N*-oxyl radical (1.27 g, 8.16 mmol, 1.20 equiv.), Cu dust (453 mg, 7.14 mmol, 1.05 equiv.), $Cu(OTf)_2$ (25 mg, 0.07 mmol, 0.01 equiv.), (4,4′-di-*tert*-butyl)-2,2′-bipyridine (73 mg, 0.27 mmol, 0.04 equiv.) and benzene (16 mL) were heated for 15 h at 75 °C in a sealed tube under an argon atmosphere. The mixture was then allowed to cool to room temperature, filtered over a thin pad of $SiO_2$ and washed with DCM. Evaporation of the solvents in vacuo and purification by flash chromatography (methyl *tert*-butyl ether/pentane 1:10) yielded **2** (1.83 g, 85%) as colourless solid. MP: 95 °C. IR (neat, $cm^{-1}$): 2976s, 2933s, 1599w, 1443s, 1374s, 1306w, 1249m, 1173w, 1128m, 1052m, 981w, 928m, 892m, 858m, 821m, 745s. $^1H$ NMR (300 MHz, $CDCl_3$): $\delta = 7.83$–7.80 (m, 3H, Ar–H), 7.72 (s, 1H, Ar–H), 7.45 (3H, Ar–H), 4.63 (q, 1H, $^3J = 6.7$ Hz, C*H*$CH_3$), 1.56 (d, 3H, $^3J = 6.7$ Hz, CHC*H*$_3$), 1.54–1.04 (m, 15H, 3 × $CH_3$, 3 × $CH_2$), 0.62 (br s, 3H, $CH_3$). $^{13}C$ NMR (75 MHz, $CDCl_3$): $\delta = 142.8$ (C), 132.8 (C), 132.2 (C), 127.5 (CH), 127.3 (CH), 127.2 (CH), 125.3 (CH), 124.9 (CH), 124.7 (CH), 124.5 (CH), 83.0 (CH), 59.3

(C), 59.2 (C), 39.9 (2 × $CH_2$), 33.9 ($CH_3$), 33.7 ($CH_3$), 23.2 ($CH_3$), 19.9 (2 × $CH_3$), 17.6 ($CH_2$). MS ($ESI^+$): 312 ($[M+H]^+$). HRMS ($ESI^+$), calcd for $[M+H]^+$: 312.2322; found: 312.2315. Anal. Calcd for $C_{21}H_{29}NO$: C, 80.98; H, 9.38; N, 4.50. Found: C, 80.76; H, 9.32; N, 4.30.

### 3.2.2. Typical procedure for the nitroxide-mediated polymerization of styrene with the initiator **2**

Alkoxyamine **2** (27 mg, 87 μmol, 1.00 equiv.) was dissolved in styrene (1.00 mL, 8.70 mmol, 100 equiv.). The solution was degassed in three freeze–thaw cycles. The reaction mixture was sealed under argon and was heated to 125 °C for 24 h. The polymerization was stopped upon cooling to room temperature and the polymer was dissolved in DCM. The solution was poured into a Petri dish and the residual monomer was removed in a vacuum-drying cabinet at elevated temperature (60 °C) for 12 h. Conversion was determined gravimetrically (642 mg, 72%); molecular weight and polydispersity index were determined by size exclusion chromatography (SEC) ($M_n = 6200$ g/mol, PDI = 1.19).

### 3.2.3. 1-[1-(4-Bromo-phenyl)-ethoxy]-2,2,6,6-tetramethyl-piperidine (**5**)

1-Bromo-4-(1-bromo-ethyl)-benzene **4** (8.31 g, 31.5 mmol, 1.00 equiv.), 2,2,6,6-tetramethylpiperidin-4-methoxy-*N*-oxyl radical (5.95 g, 38.1 mmol, 1.21 equiv.), Cu powder (2.10 g, 33.0 mmol, 1.05 equiv.), $Cu(OTf)_2$ (116 mg, 0.32 mmol, 0.01 equiv.) and (4,4′-di-*tert*-butyl)-2,2′-bipyridine (336 mg, 1.25 mmol, 0.04 equiv.) were dissolved in benzene (45 mL) and heated for 17 h at 75 °C under an argon atmosphere. The mixture was allowed to cool to room temperature, filtered over $SiO_2$ and washed with DCM. Evaporation of the solvents in vacuo and purification by flash chromatography (methyl *tert*-butyl ether/pentane 1:15) yielded **5** (9.18 g, 86%) as a colourless solid. MP: 30 °C. IR (neat, $cm^{-1}$): 3006s, 2935s, 2869s, 1483s, 1376s, 1359s, 1061s, 1010m, 925s, 835s. $^1H$ NMR (300 MHz, $CDCl_3$): $\delta = 7.44–7.41$ (m, 2H, Ar–H), 7.20–7.18 (m, 2H, Ar–H), 4.75 (q, 1H, $^3J = 6.7$ Hz, C*H*$CH_3$), 1.45 (d, 3H, $^3J = 6.7$ Hz, CHC*H*$_3$), 1.44–1.03 (15H, 3 × $CH_3$, 3 × $CH_2$), 0.67 (br s, 3H, $CH_3$). $^{13}C$ NMR (75 MHz, $CDCl_3$): $\delta = 145.6$ (C), 131.9 (2 × CH), 129.2 (2 × CH), 121.2 (C), 83.3 (CH), 60.5 (2 × C), 41.0 (2 × $CH_2$), 35.0 (2 × $CH_3$), 24.2 ($CH_3$), 21.0 (2 × $CH_3$), 17.9 ($CH_2$). MS ($ESI^+$): 340 ($[M+H]^+$). HRMS ($ESI^+$) calcd for $[M+H]^+$: 340.1271; found: 340.1269. Anal. Calcd for $C_{17}H_{26}BrNO$: C, 60.00; H, 7.70; N, 4.12. Found: C, 60.24; H, 7.75; N, 3.86.

### 3.2.4. 4-[1-(2,2,6,6-Tetramethyl-piperidin-1-yloxy)-ethyl]-benzaldehyde (**A**)

*N*-Butyl-lithium (1.6 M in hexane, 25 mL, 40 mmol, 1.5 equiv.) was slowly added to a solution of **5** (9.18 g, 27.0 mmol, 1.00 equiv.) in THF (92 mL) at −78 °C. The reaction mixture was stirred at this temperature for 1 h and DMF (10.5 mL, 135 mmol, 5.00 equiv.) was then added. The mixture was allowed to warm to room temperature for 3 h and the reaction was stopped upon addition of $NH_4Cl$ (*aq. sat*, 14 mL). The aqueous phase was extracted with $Et_2O$ (3 × 15 mL). The combined organic layers were dried over $MgSO_4$. Purification by flash chromatography (methyl *tert*-butyl ether/pentane 1:20) yielded the desired aldehyde **A** (5.97 g, 20.6 mmol, 76%) as a colourless solid.

### 3.2.5. {4-[1-(2,2,6,6-Tetramethyl-piperidin-1-yloxy)-ethyl]-phenyl}-methanol (**B**)

Aldehyde **A** (1.06 g, 3.66 mmol, 1.00 equiv.) and $LiAlH_4$ (104 mg, 2.74 mmol, 2.99 equiv.) were dissolved in THF (20 mL) and stirred for 18 h at room temperature. The reaction was stopped by adding water (116 μL) and then stirred for 5 min at room temperature. After addition of NaOH (*aq.* 15%, 116 μL) the mixture was stirred for 5 min. Then water (232 μL) was added and the suspension was stirred for additional 20 min. The white suspension was filtered and the filtrate was dried over $MgSO_4$. Evaporation of the solvents in vacuo yielded the desired alcohol **B** (1.05 g, 3.60 mmol, 98%) as a colourless oil.

### 3.2.6. 1-[1-(4-Bromomethyl-phenyl)-ethoxy]-2,2,6,6-tetramethyl-piperidine (**6**)

Alcohol **B** (5.88 g, 20.2 mmol, 1.00 equiv.) and $CBr_4$ (10.7 g, 32.3 mmol, 1.60 equiv.) were dissolved in DCM (106 mL). Triphenyl phosphine (8.51 g, 32.4 mmol, 1.60 equiv.) was added in portions over a period of 30 min at 0 °C. The reaction mixture was then stirred for 3 h at room temperature. Evaporation of the solvent in vacuo and purification by flash chromatography (methyl *tert*-butyl ether/pentane 1:20) yielded **6** (5.48 g, 15.5 mmol, 77%) as a colourless solid. IR (neat, $cm^{-1}$): 2972s, 2930s, 1452s, 1361s, 1283w, 1227s, 1133m, 1062s, 1019w, 990w, 934s, 882w, 838m, 792w. $^1H$ NMR (300 MHz, $CDCl_3$): $\delta = 7.35–7.26$ (m, 4H, Ar–H), 4.79 (q, 1H, $^3J = 6.7$ Hz, C*H*$CH_3$), 4.50 (s, 2H, $CH_2Br$), 1.47 (d, 3H, $^3J = 6.7$ Hz, CHC*H*$_3$), 1.46–1.05 (m, 15H, 3 × $CH_3$, 3 × $CH_2$), 0.68 (br s, 3H, $CH_3$). $^{13}C$ NMR (75 MHz, $CDCl_3$): $\delta = 146.6$ (C), 136.6 (C), 129.1 (2 × CH), 127.4 (2 × CH), 83.1 (CH), 60.1 (2 × C), 40.8 (2 × $CH_2$), 35.0 (2 × $CH_3$), 34.0 ($CH_2$), 23.8 ($CH_3$), 20.7 (2 × $CH_3$), 17.6 ($CH_2$). MS ($ESI^+$): 354 ($[M+H]^+$). HRMS ($ESI^+$) calcd for $[M+H]^+$: 354.1427; found: 354.1440. Anal. Calcd for $C_{18}H_{28}BrNO$: C, 61.02; H, 7.97; N, 3.95. Found: C, 60.96; H, 8.16; N, 3.88.

### 3.2.7. (2*S*,4*R*)-4-{4-[1-(2,2,6,6-Tetramethyl-piperidin-1-yloxy)-ethyl]-benzyloxy}-pyrrolidine-1,2-dicarboxylic acid 1-tert-butyl ester 2-methyl ester (**8**)

Sodium hydride (60% in mineral oil, 128 mg, 3.19 mmol, 2.50 equiv.) was added slowly to a solution of (2*S*,4*R*)-1-*tert*-butoxycarbonyl-4-hydroxy-2-methoxycarbonyl-pyrrolidine (**7**) (313 mg, 1.28 mmol, 1.05 equiv.) in DMF (7 mL) while cooling to 0 °C. The mixture was allowed to warm to room temperature for 30 min. Then a solution of **6** (431 mg, 1.22 mmol, 1.00 equiv.) in DCM (2 mL) was added and the reaction mixture was stirred for 20 h at room temperature. The reaction was stopped upon addition of water (2 mL). The aqueous phase was extracted with $Et_2O$ (3 × 2 mL) and dried over $MgSO_4$. Purification by flash chromatography (methyl *tert*-butyl ether/pentane 1:10) yielded the desired ether **8** (273 mg, 0.53 mmol, 44%)

as a racemic mixture of both diastereoisomers (ratio = 1:1). IR (neat, $cm^{-1}$): 2974s, 2932s, 1751m, 1700s, 1453w, 1396s, 1363m, 1258m, 1159s, 1091s, 1020w, 989w, 934m, 894w, 822m, 769w, 735s, 702w. $^1H$ NMR (300 MHz, $CDCl_3$): mixture of both diastereoisomers: $\delta = 7.28–7.23$ (m, 4H, Ar–H), 4.79–4.77 (m, 1H, C*H*$CH_3$), 4.45–4.43 (m, 3H, $OCH_2$, OCH), 4.18–4.08 (m, 1H, C*H*$CO_2CH_3$), 3.72–3.55 (m, 5H, $OCH_3$, C*H*$_2$CHC$O_2CH_3$), 2.32–2.28 (m, 2H, $CH_2N$), 1.47–1.03 (m, 27H, $7 \times CH_3$, $3 \times CH_2$), 0.67 (br s, 3H, $CH_3$). $^{13}C$ NMR (75 MHz, $CDCl_3$): mixture of both diastereoisomers: $\delta =$ 180.2 ($4 \times C$), 145.5 (C), 145.4 (C), 136.1 ($2 \times C$), 127.3 ($4 \times CH$), 126.7 ($2 \times CH$), 126.6 ($2 \times CH$), 82.8 ($2 \times CH$), 80.1 (C), 80.0 (C), 75.9 ($2 \times CH$), 71.1 ($CH_2$), 71.0 ($CH_2$), 59.7 ($4 \times C$), 58.0 (CH), 57.8 (CH), 52.1 ($CH_3$), 51.9 ($CH_3$), 51.4 ($CH_2$), 51.3 ($CH_2$), 40.4 ($4 \times CH_2$), 36.7 ($2 \times CH_2$), 34.2 ($2 \times CH_3$), 34.1 ($2 \times CH_3$), 28.4 ($3 \times CH_3$), 28.3 ($3 \times CH_3$), 23.5 ($2 \times CH_3$), 20.4 ($2 \times CH_2$), 20.3 ($2 \times CH_2$), 17.2 ($2 \times CH_2$). MS ($ESI^+$): 541 ($[M + Na]^+$), 519 ($[M + H]^+$). HRMS ($ESI^+$), calcd for $[M + H]^+$: 519.3429; found: 519.3418. Anal. Calcd for $C_{29}H_{46}N_2O_6$: C, 67.15; H, 8.94; N, 5.40. Found: C, 66.90; H, 8.88; N, 5.24.

### *3.2.8. (2S,4R)-4-{4-[1-(2,2,6,6-Tetramethyl-piperidin-1-yloxy)-ethyl]-benzyloxy}-pyrrolidine-1,2-dicarboxylic acid 1-tert-butyl ester (**9**)*

NaOH (*aq*., 2%, 10 mL) was added to a solution of **8** (367 mg, 0.707 mmol, 1.00 equiv.) in methanol (60 mL). The reaction mixture was stirred for 64 h at room temperature. Sulfuric acid (*aq*., 50%) was then added to adjust the pH to 4. The aqueous phase was extracted with methyl *tert*-butyl ether ($3 \times 15$ mL). The combined organic layers were dried over $MgSO_4$. Evaporation of the solvents in vacuo and purification by flash chromatography (methanol/$CH_2Cl_2$ 1:15) yielded **9** (234 mg, 0.464 mmol, 66%, 1:1 mixture of both diastereoisomers) as a colourless solid. IR (neat, $cm^{-1}$): 2975s, 2931s, 1699s, 1396s, 1365s, 1209w, 1258m, 1161s, 1131m, 1092s, 1063s, 1019m, 935m, 822m, 770m, 703m. $^1H$ NMR (400 MHz, $CDCl_3$): mixture of both diastereoisomers: $\delta = 8.42$ (br s, 1H, $CO_2H$), 7.27–7.26 (m, 4H, Ar–H), 4.81–4.79 (m, 1H, C*H*$CH_3$), 4.50–4.37 (m, 3H, $OCH_2$, CHO), 4.18–4.11 (m, 1H, C*H*$CO_2CH_3$), 3.74–3.55 (m, 2H, C*H*$_2$CHC$O_2CH_3$), 2.44–2.13 (m, 2H, $CH_2N$), 1.47–1.02 (m, 27H, $7 \times CH_3$, $3 \times CH_2$), 0.68 (br s, 3H, $CH_3$). $^{13}C$ NMR (75 MHz, $CDCl_3$): mixture of both diastereoisomers: $\delta = 180.6$ ($2 \times C$), 178.3 ($2 \times C$), 145.8 ($2 \times C$), 136.5 ($2 \times C$), 127.5 ($2 \times CH$), 127.3 ($2 \times CH$), 126.6 ($4 \times CH$), 83.2 ($2 \times CH$), 80.9 ($2 \times C$), 76.4 ($2 \times CH$), 71.6 ($CH_2$), 71.4 ($CH_2$), 60.2 ($4 \times C$), 58.5 ($2 \times CH$), 52.4 ($CH_2$), 51.8 ($CH_2$), 40.6 ($4 \times CH_2$), 37.0 ($2 \times CH_2$), 35.0 ($2 \times CH_3$), 34.5 ($2 \times CH_3$), 28.8 ($3 \times CH_3$), 28.7 ($3 \times CH_3$), 24.0 ($2 \times CH_3$), 20.8 ($4 \times CH_3$), 17.6 ($2 \times CH_2$). MS ($ESI^+$): 527 ($[M + Na]^+$), 505 ($[M + H]^+$). HRMS ($ESI^+$), calcd for $[M + H]^+$: 505.3272; found: 505.3282.

### *3.2.9. (2S,4R)-4-{4-[1-(2,2,6,6-Tetramethyl-piperidin-1-yloxy)-ethyl]-benzyloxy}-pyrrolidine-2-carboxylic acid (**10**)*

The protected amino acid **8** (273 mg, 0.53 mmol, 1.00 equiv., 1:1 mixture of the two isomers) was dissolved in DCM (1 mL). Trifluoroacetic acid (400 μL, 5.15 mmol, 9.5 equiv.) was added and the solution was stirred for 4 h at room temperature. The solvent was then evaporated under reduced pressure. The residue was dissolved in ethyl acetate and washed with $NaHCO_3$ (*aq*. *sat*, $3 \times 5$ mL). The organic layer was dried over $MgSO_4$. Evaporation of the solvents in vacuo yielded the crude product which was dissolved in methanol (50 mL) and NaOH (*aq*., 2%, 7 mL). The reaction mixture was stirred for 16 h at room temperature. Evaporation of the solvents in vacuo and purification by cation exchange chromatography (*Dowex 50 X 8*, 50–100 mesh, eluent: $NH_3$ (*aq*., 5%)) yielded **10** (210 mg, 0.52 mmol, 98%, 1:1 mixture of both diastereoisomers) as a colourless solid. MP: 95 °C. IR (neat, $cm^{-1}$): 3374m, 2973s, 2930s, 2871w, 1617s, 1515w, 1443w, 1361s, 1259w, 1210m, 1131w, 1061s, 987w, 933m, 882w, 821s, 789w. $^1H$ NMR (300 MHz, $CD_3OD$): mixture of both diastereoisomers: $\delta = 7.35$ (m. 4H, Ar–H), 4.59–4.01 (m, 4H, C*H*$CH_3$, $OCH_2$, CHO), 3.56–3.26 (m, 3H, C*H*$CO_2H$, C*H*$_2$CHC$O_2H$), 2.62–2.10 (m, 2H, $CH_2N$), 1.49–0.69 (m, 21H, $5 \times CH_3$, $3 \times CH_2$). $^{13}C$ NMR (75 MHz, $CD_3OD$): mixture of both diastereoisomers: $\delta = 177.8$ ($2 \times C$), 146.7 (C), 146.5 (C), 137.8 ($2 \times C$), 128.9 ($2 \times CH$), 128.8 ($2 \times CH$), 127.9 ($2 \times CH$), 127.7 ($2 \times CH$), 84.3 ($2 \times CH$), 79.1 (CH), 78.0 (CH), 71.9 ($CH_2$), 71.6 ($CH_2$), 61.6 (CH), 61.4 (CH), 60.9 ($4 \times C$), 52.1 ($2 \times CH_2$), 41.5 ($4 \times CH_2$), 36.6 ($2 \times CH_2$), 35.6 ($4 \times CH_3$), 23.9 ($2 \times CH_3$), 21.1 ($4 \times CH_3$), 18.2 ($2 \times CH_2$). MS ($ESI^+$): 427 ($[M + Na]^+$), 405 ($[M + H]^+$). HRMS ($ESI^+$), calcd for $[M + H]^+$: 405.2748; found: 405.2752.

### *3.2.10. Typical procedure for the nitroxide-mediated polymerization of styrene with the initiator **9***

Alkoxyamine **9** (93 mg, 89 μmol, 1.00 equiv.) was dissolved in styrene (1.00 mL, 8.90 mmol, 100 equiv.). The solution was degassed in three freeze–thaw cycles. The reaction mixture was sealed under argon and was heated to 125 °C for 12 h. The polymerization was stopped upon cooling to room temperature and the polymer was dissolved in DCM. The solution was poured into a Petri dish and the residual monomer was removed in a vacuum-drying cabinet at elevated temperature (60 °C) for 12 h. Conversion was determined gravimetrically (799 mg, 86%); molecular weight and polydispersity index were determined by size exclusion chromatography (SEC) ($M_n = 8100$ g/mol, PDI = 1.18).

### *3.2.11. Synthesis of the deprotected proline–polymer conjugate **11***

Trifluoroacetic acid (1.8 mL, 23 mmol, 125 equiv.) was added to a solution of the polymer-bound catalyst prepared using initiator **9** (1.83 g, $M_n = 9900$ g/mol, 184 μmol, 1.00 equiv.) in DCM (30 mL). The mixture was stirred for 4 h at room temperature and was then stopped upon addition of water (20 mL). The aqueous phase was extracted with DCM ($3 \times 20$ mL). The combined organic layers were washed with $NaHCO_3$ (*aq*. *sat*, $3 \times 20$ mL) and water ($2 \times 30$ mL) and dried over $MgSO_4$. Evaporation of the solvents in vacuo yielded **11** (1.61 g, 134 μmol, 89%) as a colourless solid.

IR (neat, $cm^{-1}$): 3060m, 3026m, 2924s, 2851m, 2362w, 2337w, 1946w, 1873m, 1601m, 1492s, 1451s, 1375m, 1265m, 1222m, 1157s, 741s, 697s.

### 3.3. Electrospinning of nanofibers

We applied for the electrospinning of the polystyrene fibers containing either the chromophore species or the catalysts a strong electric field of the order of $10^3$ V/cm to the droplet of the polymer solution emerging from a cylindrical die. The electric charges which are accumulated on the surface of the droplet cause droplet deformation along the field direction, even though the surface tension counteracts droplet evolution. In supercritical electric fields the field strength overcomes the surface tension and a fluid jet emanates from the droplet tip. The jet is accelerated towards the counter electrode. During this transport phase the jet is subjected to strong electrically driven circular bending motions which cause a strong elongation and thinning of the jet, to a solvent evaporation until the solid nanofiber is deposited on the counter electrode. Electrospinning has, for the case considered here, the additional distinct advantages that the catalytic species can be incorporated into the nanofibers during the electrospinning process, porous fibers can be produced enhancing the surface area and various types of fiber arrangements in space become available allowing to control the permeability of such nonwoven membranes.

Polystyrene (1.000 g, $M_n = 150\,000-300\,000$ g/mol) and oligostyrene (0.100 g) were dissolved in dimethylacetamide (DMAc) (4.2 mL). The solution, stored within a reservoir, was pumped through a metal capillary connected with a voltage supply using a peristaltic pump. The circular orifice of the capillary had a diameter of 0.45 mm. A circular shaped counter electrode with a diameter of 18 cm was located below the reservoir, so that a vertical arrangement of the electrodes resulted. Fibers were collected on aluminum foil. The distance between the tip of the capillary and the counter electrode was typically of the order of 15 cm and the applied voltage was 20 kV.

### 3.4. Typical procedure of leaching measurements

Chromophore-modified oligostyrene ($1.1 \times 10^{-7}$ mol fluorescent end groups), respectively, polystyrene films and fibers containing 9 wt% oligostyrene ($1.1 \times 10^{-7}$ mol fluorescent end groups) were immersed in 10 mL DMSO. The resulting solution was used directly for measurement of the fluorescence intensity as a function of immersion time.

## 4. Results and discussions

### 4.1. Synthesis of naphthalene and proline conjugated oligostyrenes as model systems for leaching studies

As chromophore we chose the naphthyl moiety. The nitroxide-mediated radical polymerization [19] of styrene allows careful adjusting of the length of the chromophore conjugated polystyrene. The alkoxyamine initiator/regulator **2**, which is able to control the polymerization of styrene, was readily prepared from commercially available 2-ethylnapthalene. Bromination of 2-ethylnaphthalene under irradiation provided bromide **1**, which was transformed to the alkoxyamine **2** in a good yield via a Cu-catalyzed alkoxyamine formation using TEMPO (2,2′,6,6′-tetramethylpiperidine-1-oxyl radical, Scheme 1) [20]. Controlled radical polymerizations were performed in neat styrene at 125 °C for 24 h. Conversion was determined gravimetrically; molecular weight and polydispersity index (PDI) were determined by size exclusion chromatography (SEC). Results of representative polymerizations are presented in Table 1. As can be seen in entries 1–4, the length of the naphthalene-conjugated polystyrene can be controlled by the amount of added initiator **2**. Naphthalene-conjugated polystyrenes with $M_n$ of 2800, 4100, 4400, 5100, 6400, 8200, 10 700, 12 400 and 15 200 g/mol with PDIs of around 1.2 were isolated.

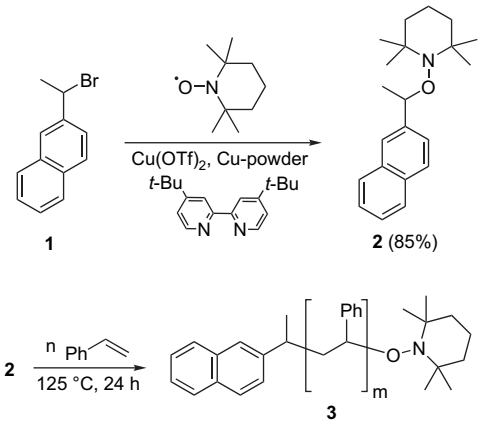


Scheme 1. Synthesis of naphthalene-conjugated alkoxyamine **3**.

Proline modified polystyrenes were prepared in a multistep synthesis. Bromination of 4-ethylbromobenzene with $Br_2$ under irradiation using visible light gave the benzylic bromide **4** which was subsequently transformed into the corresponding TEMPO-derived alkoxyamine **5** using Cu catalysis (86%, Scheme 2). Formylation, lithium aluminium hydride (LAH) reduction and benzylic bromination afforded bromide **6** in a good overall yield (57%). Etherification under standard conditions using bromide **6** and the protected hydroxy-L-proline **7** yielded alkoxyamine **8** (44%). Alkoxyamine **8** was isolated as a 1:1 mixture of diastereoisomers. The corresponding acid **9** was readily obtained upon saponification. Double deprotection

Table 1
Synthesis of naphthalene labeled polystyrene

| Entry | Alkoxyamine **2** (mol%) | Conversion (%) | $M_{n,theo}$ (g/mol) | $M_{n,exp}$ (g/mol) | PDI |
|---|---|---|---|---|---|
| 1 | 0.58 | 68 | 12 400 | 11 800 | 1.21 |
| 2 | 1.0 | 72 | 8200 | 6200 | 1.19 |
| 3 | 1.5 | 65 | 5100 | 4300 | 1.20 |
| 4 | 2.0 | 69 | 4100 | 3300 | 1.20 |

$M_{n,theor}$ = theoretical number average molecular weight calculated from the conversion and the alkoxyamine concentration. $M_n$ = number average molecular weight. PDI = polydispersity index.

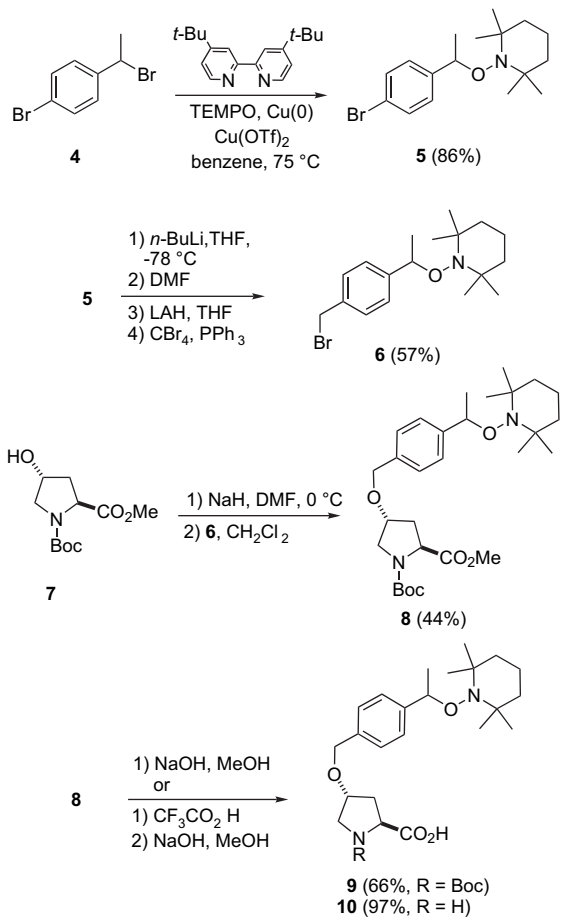


Scheme 2. Synthesis of alkoxyamines **8**–**10** (Boc = *tert*-butyloxycarbonyl).

and purification using ion exchange chromatography provided the free amino acid **10** in an excellent yield.

The first polymerization experiments were conducted using the fully deprotected amino acid **10** as a regulator/initiator. The polymerizations were performed in neat styrene using **10** (0.5–2.0 mol%) at 125 °C (Table 2). We found that polymerizations were very fast with this initiator for most of the experiments. However, polymerizations initiated with **10** were difficult to control and results were not reproducible (compare entries 2 and 3). Moreover, $M_{n,theor}$ and $M_n$ determined by GPC often varied to a large extent showing that initiation with **10** is not efficient (entries 1 and 2). In addition, PDIs above 1.5 were often obtained for the **10**-initiated polymerizations (results not shown). Probably the free amino acid functionalities do interfere with the polymerization process. In fact it is known that acids as additives influence the nitroxide-mediated polymerization [21]. Therefore, we repeated the styrene polymerization with the fully protected alkoxyamine **8**. Pleasingly, well controlled polymerizations were achieved using this initiator and results could be well reproduced and PDIs were small (entries 6–8). As expected, without the free acid functionality, the polymerization occurred far slower. A reaction time of 24 h was necessary in order to get high conversions. However, we faced serious problems in the deprotection (saponification and Boc-deprotection) of the L-proline-conjugated polystyrene. Therefore, we switched to the Boc-protected alkoxyamine **9** bearing the free acid as initiator (Scheme 3). We were pleased to find that polymerizations using **9** were controlled and reproducible. Some representative results are given in entries 9–11. Moreover, Boc-deprotection after polymerization to give polystyrene-L-proline conjugate **11** was readily achieved with $CF_3COOH$ in $CH_2Cl_2$ at room temperature.

Table 2
Controlled styrene polymerization using alkoxyamines **8**–**10**

| Entry | **8**, **9** or **10** (mol%) | Conversion (%) | Time (h) | $M_{n,theo}$ (g/mol) | $M_{n,exp}$ (g/mol) | PDI |
|---|---|---|---|---|---|---|
| 1 | **10** (0.50) | 69 | 4 | 14 800 | 38 800 | 1.30 |
| 2 | **10** (0.60) | 70 | 4 | 12 600 | 40 000 | 1.29 |
| 3 | **10** (0.60) | 61 | 4.5 | 10 600 | 9800 | 1.19 |
| 4 | **10** (0.70) | 67 | 4 | 10 300 | 15 300 | 1.30 |
| 5 | **10** (0.80) | 70 | 4.5 | 9500 | 11 400 | 1.17 |
| 6 | **8** (0.79) | 76 | 24 | 10 000 | 12 100 | 1.12 |
| 7 | **8** (0.82) | 74 | 24 | 9400 | 13 000 | 1.12 |
| 8 | **8** (0.81) | 73 | 24 | 9400 | 12 600 | 1.14 |
| 9[a] | **9** (0.99) | 85 | 14 | 9400 | 9300 | 1.21 |
| 10[a] | **9** (0.99) | 86 | 12 | 9000 | 8100 | 1.18 |
| 11[a] | **9** (0.98) | 69 | 8 | 7300 | 6800 | 1.20 |

[a] GPC analysis was performed prior to the deprotection.

### 4.2. Nanofiber preparation and properties

To obtain the nonwoven composed of PS fibers we performed electrospinning using tetrahydrofuran, chloroform, dichloromethane and *N*,*N*-dimethylacetamide solutions containing polystyrene in the concentration range from 5 wt% up to 20 wt%. The observation is that spinning solutions with lower concentrations of polystyrene resulted in fibers on which beads were superimposed.

Nanofibers containing either the oligostyrene-modified chromophores **3** or the oligostyrene-modified proline **11** were spun from DMAc solution. Again it was possible to obtain nanofibers free of beads. These are shown in Fig. 1a and b. The total porosity of such nonwovens is about 90%. The diameter of the fibers amounts to about 0.8 μm and the fibers are free of beads.

The inclusion of the oligomer species into the polystyrene matrix may result in a strong softening of the fibers since the oligostyrene may act as a plasticizer reducing, for instance, the glass transition temperature. A further possibility is that the oligostyrene-modified compounds perform an aggregation or

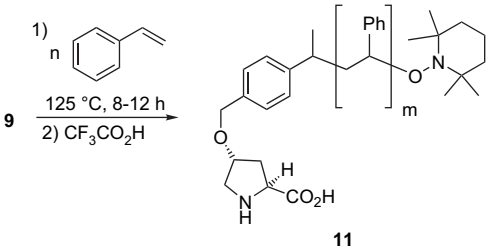


Scheme 3. Polymerization of styrene using alkoxyamine **9** as initiator regulator with subsequent Boc-deprotection.

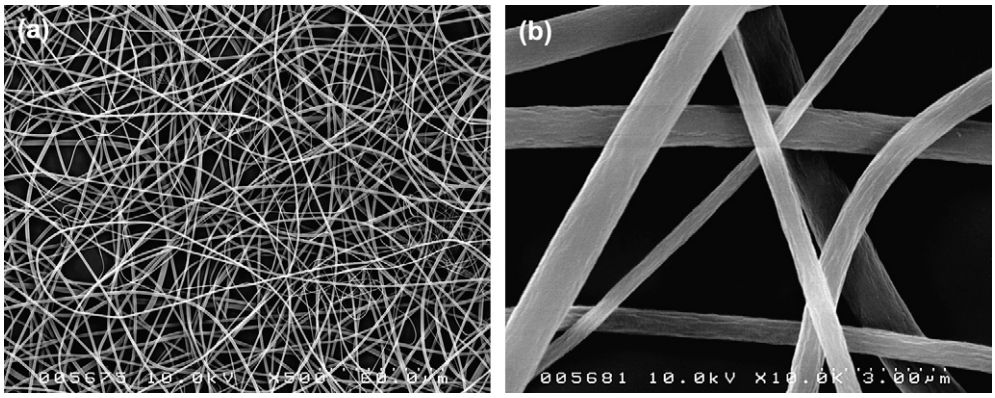


Fig. 1. SEM images of composite fibers prepared via electrospinning from DMAc solution containing polystyrene and the oligostyrene-modified proline catalyst **11**.

even phase separation possibly also a crystallization. To evaluate such possible features we have performed both calorimetric and X-ray studies.

### 4.3. X-ray investigation

X-ray measurements show that the synthesized oligostyrenes are amorphous displaying a structured halo corresponding clearly to the one known for polystyrene. The fact that the oligostyrenes are not able to crystallize enhances their miscibility in the polystyrene matrix considerably even for higher concentrations. The polystyrene matrix containing the oligostyrene compound shows a similar scattering diagram as the pure components as expected.

### 4.4. DSC studies

The oligostyrene-modified proline model systems show in thermal analysis just a stepwise increase of the specific heat at a temperature of about 85 °C what is a signature of the onset of a glass transition (Fig. 2). These results are in agreement with those obtained by X-ray analysis showing the oligostyrenes to be amorphous. Mixtures of the polystyrene matrix with the oligostyrene display a single $T_g$ increasing linearly with increasing polystyrene content (Fig. 3) indicating that the oligostyrene is homogeneously mixed.

### 4.5. Solubility of the oligostyrene-modified chromophores

The oligostyrene-modified chromophores **3** served the purpose to determine the solubility–chain length dependence characteristic of oligostyrene in the selected solvent DMSO as well as in the polystyrene matrix of high molecular weight. The methods of choice are absorption and fluorescence spectroscopies. Fig. 4a shows the spectra of the different chromophore species in THF and Fig. 4b the corresponding fluorescence spectra normalized to a given mass concentration. The spectra show two absorption bands. A comparison of the spectra of polystyrene and chromophore functionalized oligostyrenes reveals that the lower energy band with a maximum at 291 nm corresponds to the chromophore end group.

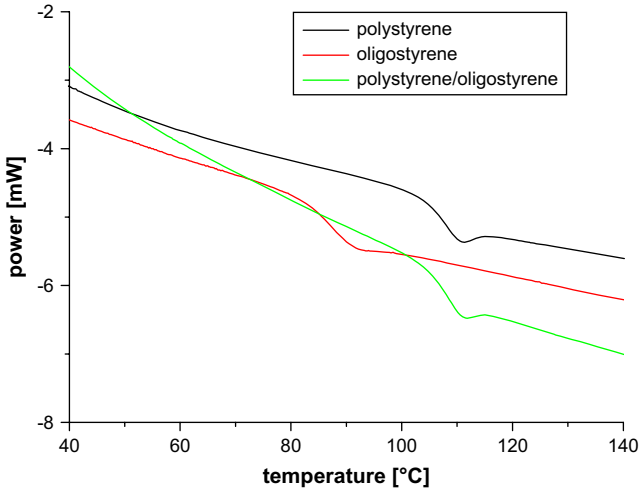


Fig. 2. DSC results for polystyrene, oligostyrene and a mixture containing 9 wt% oligostyrene.

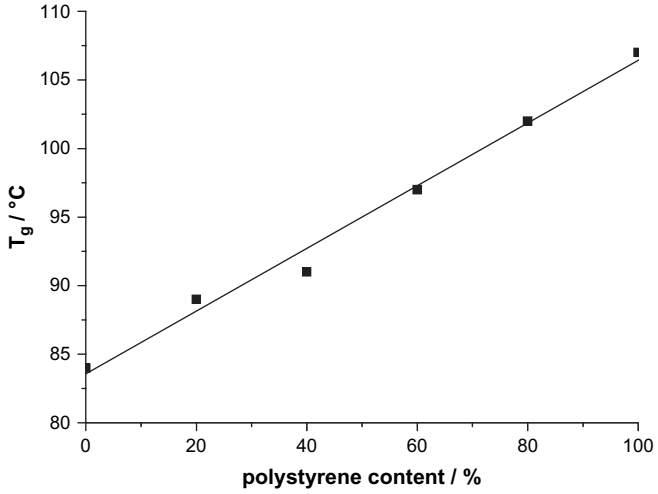


Fig. 3. Glass transition temperature of polystyrene–oligostyrene mixtures as a function of polystyrene content.

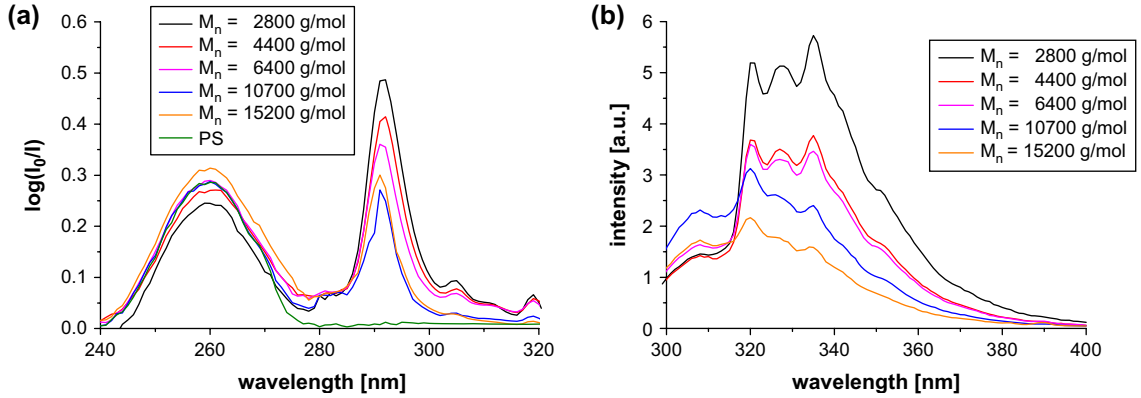


Fig. 4. (a) Absorption and (b) fluorescence spectra (excitation wavelength: 291 nm) of polystyrene and of the oligostyrene-modified chromophores **3** for various chain lengths in THF.

THF was chosen due to its good solubility for the compounds studied here. It is apparent that the spectra are modified to a certain extent by the attachment of the chromophores to the oligostyrene chain and that they also depend on the chain length. This is not surprising, for instance, for the fluorescence spectra in view of the fact that styrene displays fluorescence in THF. Similar spectra were obtained in the solvent DMSO, yet spectra could only be obtained for small concentrations (see below) particularly for longer oligostyrene chains.

These magnitudes of the absorption and fluorescence spectra were analyzed as a function of the chromophore concentration both in terms of the peak maximum at 291 nm and of its integral value in order to obtain a calibration curve. The results for the integral values are displayed in Fig. 5. The diagrams reveal that the magnitudes increase linearly as a function of the concentration. Note that the diagrams are normalized with respect to the molar concentration of the chromophore. It is first of all apparent that the diagrams display nearly straight lines for low concentrations. In the case of the absorption spectra we expect such a linear relationship on the basis of the Lambert–Beer law. We have no explanation for the deviation of the calibration curve from a linear relationship. The fact that the fluorescence is linearly dependent on the concentrations even at higher concentrations can be taken as an indication that no aggregation effects occur at higher concentrations. It is apparent that the calibration curves do not agree completely for the various chain lengths apparently because of the modifications induced to their spectral properties by the attachment to the oligostyrene chains.

The calibration curves obtained in this way reveal that the lowest concentration of the modified chromophores which can be evaluated is of the order of $10^{-6}$ mol/L. The fluorescence spectra are not significantly modified if high molecular polystyrene is used as the solid matrix for the dispersion of the modified chromophores. This is apparent from Fig. 6, revealing these spectra. But the absorption spectra are dominated by the absorption of polystyrene.

In the next step we performed solubility studies of the modified chromophores **3** in the solvent DMSO, a solvent often used in catalysis. The oligostyrenes were dissolved until the upper limiting concentration which could be achieved and the fluorescence spectra were investigated. We furthermore determined this specific upper concentration by evaporating the solvent and a subsequent determination of the residual weight of the chromophores **3**. This was, however, only possible for the shorter chain length chromophores since the solubility of

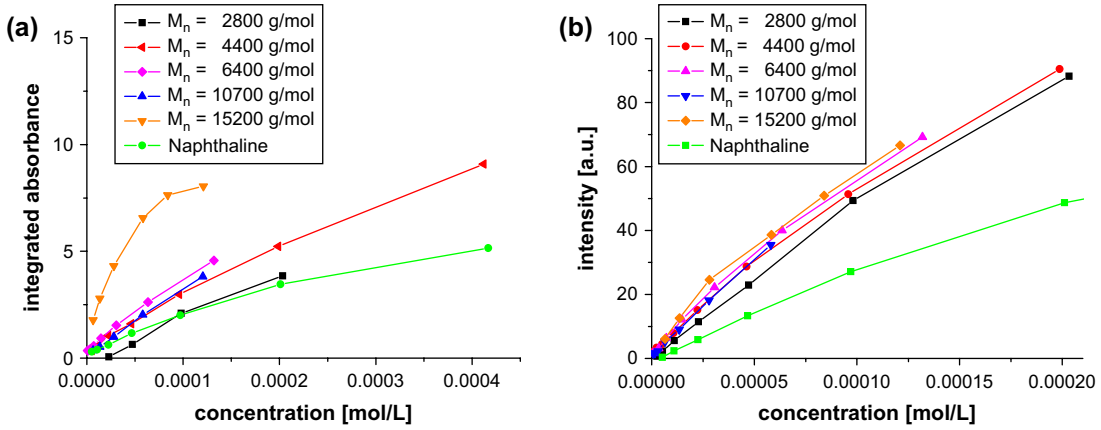


Fig. 5. Calibration curves for the dependence of the magnitude of the (a) absorption and (b) fluorescence (excitation wavelength: 291 nm) on the concentration of the oligostyrene-modified chromophores **3** for various chain lengths.

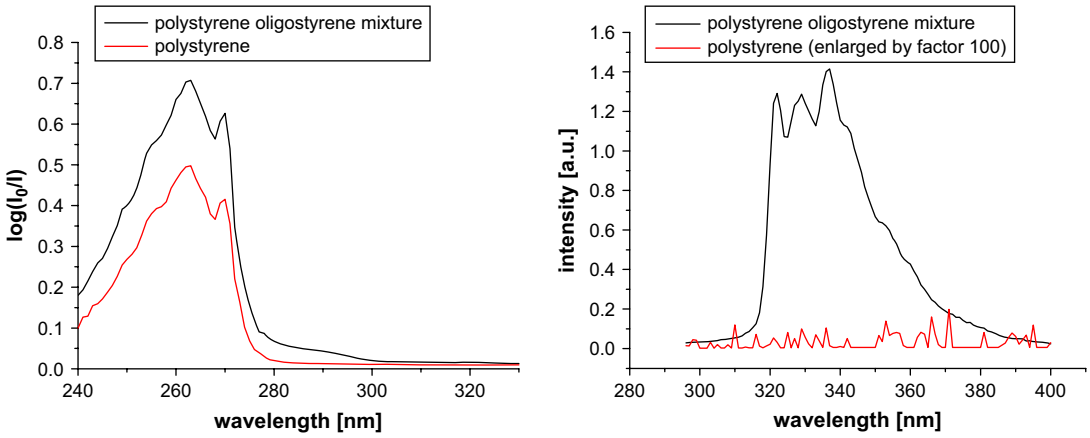


Fig. 6. Absorption and fluorescence spectra (excitation wavelength: 291 nm) of a polystyrene film and of modified chromophore **3** ($M_n = 4400$ g/mol) using high molecular weight polystyrene as matrix.

the larger chain chromophores was much too small for this approach. In any case the results obtained by these procedures are shown in Table 3.

It is readily apparent that the solubility decreases dramatically with increasing chain length as expected on the basis of theoretical considerations (see above). Several conclusions can be drawn from these results relating to the catalytic activity of a catalyst conjugated to an oligostyrene. The assumption implicit in these conclusions is that the solubility of the oligostyrene-modified proline catalysts follows approximately the same pattern. One conclusion is that the concentration of the longer chain catalyst within the reaction mixture containing DMSO will be much lower in order to induce catalytic processes for chain length larger than 4400 g/mol. Further conclusions which can be drawn relate to the upper limit of residual catalytic species in the product which can be tolerated in a given area of applications.

### 4.6. Leaching and reversed leaching studies

Oligostyrene as well as polystyrene films and nanofibers containing the oligostyrene-modified chromophores **3** were immersed in the solvent DMSO for elongated times. Spectroscopic investigations were performed on the solvent in the environment of the chromophores as a function of the immersion time. The results are displayed in Fig. 7.

The oligostyrene is dissolved readily up to a limiting concentration which corresponds to the one given in Table 3 ($\approx 10^{-7}$ mol/L). A characteristic time scale within which the limiting value is approached is of the order of 20 h. This dissolution process is strongly restricted for oligostyrene homogeneously mixed in the polystyrene fiber and film due to the much better solubility in polystyrene as compared to DMSO. The final concentration in the DMSO solution is very low, close to the limit of resolution. Importantly, chromophores with chain length above about 10 000 g/mol do not leach into the solvent at all within the accuracy of the spectroscopic evaluation. These results show that the concept of immobilization and suppression of leaching investigated here seems to function.

This becomes evenly more evident if we consider reverse leaching studies. Polystyrene nanofibers free of the chromophore **3** are immersed for such studies into a solvent composed of DMSO in which the oligostyrene-modified chromophore is dissolved. The results are shown in Fig. 8.

The intensity of the fluorescence within the DMSO solution decreases as a function of the time of contact with the nanofibers since the chromophores leach into the nanofibers. In

Table 3
Solubility of the modified chromophores **3** in DMSO as a function of the chain length of the oligostyrene chain

| $M_n$ | mol/L |
|---|---|
| 2800 | $\approx 10^{-4}$ |
| 4400 | $\approx 10^{-7}$ |
| 6400 | $\approx 10^{-8}$ |
| 10 700 | $< 10^{-8}$ |
| 15 200 | $< 10^{-8}$ |

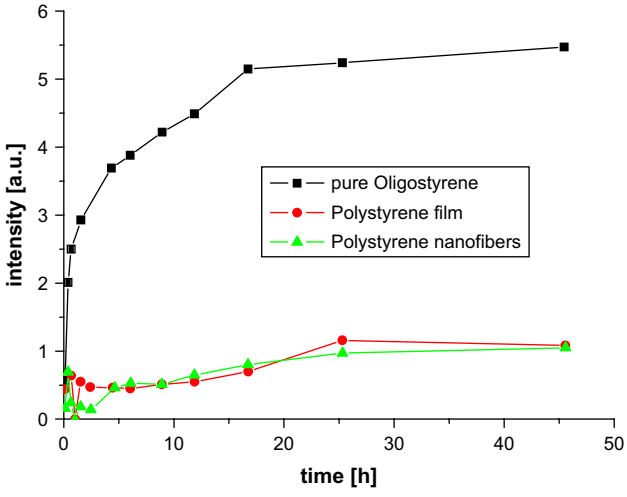


Fig. 7. Fluorescence spectra (excitation wavelength: 291 nm) obtained for the DMSO environment of the polystyrene film and polystyrene nanofibers containing oligostyrene-modified chromophores **3** ($M_n = 4400$ g/mol) as a function of the immersion time.

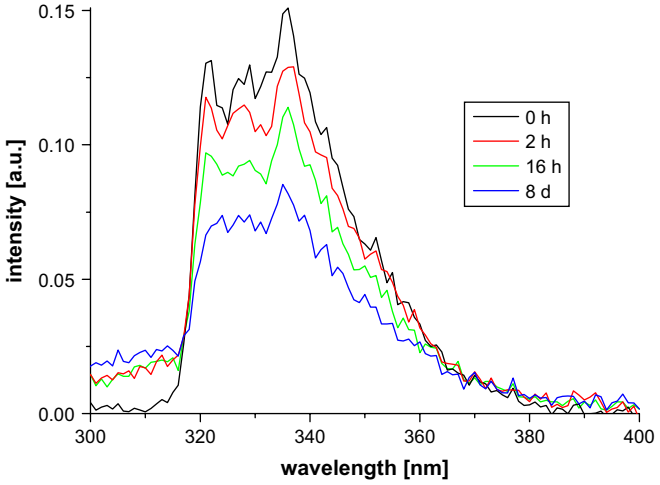


Fig. 8. Decrease in the magnitude of the fluorescence (excitation wavelength: 291 nm) of the DMSO–chromophore solution ($M_n = 4400$ g/mol) as a function of the contact time with polystyrene nanofibers.

control experiments a constant fluorescence intensity as a function of time of the DMSO–chromophore solution was observed. Further measurements on the dissolved nanofibers verified the assumption that the chromophore-modified oligostyrenes diffused into the polystyrene fibers. The obvious reason is that the chemical potential is lower for the chromophores within the polystyrene matrix as compared to the DMSO environment. These results show that the suppression of leaching of the modified chromophores into the solvent is not a kinetic but a thermodynamic phenomenon.

## 5. Conclusions

We have shown that proline–oligostyrene conjugates with well defined molecular weights and small PDIs can readily be prepared by NMP. This approach can also be used for the synthesis of naphthalene–oligostyrene conjugates. Low-molecular weight oligostyrenes can be coelectrospun with high molecular weight polystyrene (150 000–300 000 g/mol) to provide nanofibers where the oligostyrenes are well dispersed within the fibers. Aggregation of the oligostyrenes in the fibers is not observed. The diameter of the fibers can be controlled by the electrospinning process. Oligostyrenes with $M_n > 4000$ g/mol show very low solubility in DMSO. Importantly, oligostyrenes with $M_n > 10\,000$ g/mol immobilized into the polystyrene nanofibers do not leach out of the fibers into DMSO. In fact, diffusion of oligostyrene from the DMSO solution into the polystyrene nanofiber matrix is occurring for thermodynamic reasons. Due to the high surface area of the nanofibers and the well dispersed catalytic active moieties within the fibers the present system should behave as highly active immobilized catalyst system. It is important to note that the concept is general and should be applicable for any polymer which can be electrospun. The polystyrene matrix material, as used herein, should allow reactions to be conducted in DMSO, $H_2O$ and MeOH. Studies on the catalytic activity of the immobilized proline in organocatalysis in these solvents are under way and will be reported elsewhere. To broaden the solvent compatibility other matrix polymers in combination with catalyst–polymer conjugates of that given polymer will be coelectrospun and tested as immobilized catalysts in the near future.

## Acknowledgement

We gratefully acknowledge the financial support by the Deutsche Forschungsgemeinschaft within the program Organokatalyse.

## References

[1] Alexeev OS, Gates BC. Industrial and Engineering Chemistry Research 2003;42:1571–87.
[2] Blaser HU, Indolese A, Schnyder A, Steiner H, Studer M. Journal of Molecular Catalysis A: Chemical 2001;173:3–18.
[3] Jensen KF. Chemical Engineering Science 2001;56:293–303.
[4] Kobayashi S, Akiyama R. Chemical Communications 2003;4:449–60.
[5] Kobayashi S, Nagayama S. Journal of the American Chemical Society 1998;120:2985–6.
[6] For reviews, see: Clapham B, Reger TS, Janda KD Tetrahedron 2001;57:4637–62;
(a) Bailey DC, Langer SH. Chemical Reviews 1981;81:109–48;
(b) Akelah A, Sherrington DC. Chemical Reviews 1981;81:557–87.
[7] Vaeth KM, Tang CW. Journal of Applied Physics 2002;92:3447–53.
[8] Sander R, Stümpflen V, Wendorff JH, Greiner A. Macromolecules 1996;29:7705–8.
[9] Stähelin M, Walsh CA, Burland DM, Miller RD, Twieg RJ, Volksen W. Journal of Applied Physics 1993;73:8471–9.
[10] Ferry JD. Viscoelastic properties of polymers. New York: J. Wiley; 1980.
[11] Vriezema DM, Aragonès MC, Elemans JAAW, Cornelissen JJLM, Rowan AE, Nolte RJM. Chemical Reviews 2005;105:1445–89.
[12] Huang ZM, Zhang YZ, Kotaki M, Ramakrishna S. Composites Science and Technology 2003;63:2223–53.
[13] Dersch R, Greiner A, Wendorff JH. Dekker encyclopedia of nanoscience and nanotechnology. Marcel Dekker Inc.; 2004. p. 2931.
[14] Li D, Xia Y. Advanced Materials 2004;16:1151–70.
[15] Tomadakis MM, Robertson TJ. Journal of Composite Materials 2005;39:163–88.
[16] Tomadakis MM, Sotirchos SV. AIChE Journal 1991;37:74–86.
[17] Tomadakis MM, Sotirchos SV. Journal of Chemical Physics 1993;98:616–26.
[18] Stasiak M, Studer A, Greiner A, Wendorff JH. Chemistry – A European Journal 2007;13:6150–6.
[19] Hawker CJ, Bosman AW, Harth E. Chemical Reviews 2001;101:3661–88.
[20] Matyjaszewski K, Woodworth BE, Zhang X, Gaynor SG, Metzner Z. Macromolecules 1998;31:5955–7.
[21] Nilsen A, Braslau R. Journal of Polymer Science, Part A: Polymer Chemistry 2006;44:697–717.